UC San Diego
UC San Diego Previously Published Works

Title
Proton density water fraction as a biomarker of bone marrow cellularity: Validation in ex vivo spine specimens

Permalink
https://escholarship.org/uc/item/1569w96g

Journal
Magnetic Resonance Imaging, 32(9)

ISSN
0730-725X

Authors
MacEwan, Iain J
Glembotski, Nicholas E
D’Lima, Darryl
et al.

Publication Date
2014-11-01

DOI
10.1016/j.mri.2014.03.005

Peer reviewed

eScholarship.org Powered by the California Digital Library
University of California

Magnetic Resonance Imaging 32 (2014) 1097–1101

Contents lists available at ScienceDirect

Magnetic Resonance Imaging

journal homepage: www.mrijournal.com

Proton density water fraction as a biomarker of bone marrow cellularity: Validation in ex vivo spine specimens

Iain J. MacEwan [a], Nicholas E. Glembotski [b], Darryl D'Lima [b], Won Bae [c], Koichi Masuda [d], Hooman H. Rashidi [e], Loren K. Mell [a], Mark Bydder [c,*]

[a] Center for Advanced Radiotherapy Technologies, Department of Radiation Medicine and Applied Sciences, 3855 Health Sciences Dr. #0843, La Jolla, CA, USA
[b] Scripps Translational Science Institute, 3344 North Torrey Pines Court Suite 300, La Jolla, CA, USA
[c] Department of Radiology, University of California San Diego, 408 Dickinson Street, San Diego, CA, USA
[d] Skeletal Translational Research Laboratory, Department of Orthopaedic Surgery, School of Medicine, University of California, San Diego, CA, USA
[e] Department of Pathology, University of California San Diego, School of Medicine & VA Medical Center, San Diego, CA, USA

A R T I C L E I N F O

Article history:
Received 22 May 2013
Revised 23 January 2014
Accepted 7 March 2014

Keywords:
Bone marrow
Cellularity
MRI
Fat quantification

A B S T R A C T

The purpose of this study was to evaluate a magnetic resonance imaging (MRI) technique for quantifying the proton density water fraction (PDWF) as a biomarker of bone marrow cellularity. Thirty-six human bone marrow specimens from 18 donors were excised and subjected to different measurements of tissue composition: PDWF quantification using a multiple gradient echo MRI technique, three biochemical assays (triglyceride, total lipid and water content) and a histological assessment of cellularity. Results showed a strong correlation between PDWF and bone marrow cellularity from histology ($r = 0.72$). A strong correlation was also found between PDWF and the biochemical assay of water content ($r = 0.76$). These results suggest the PDWF is a predictor of bone marrow cellularity in tissues and can provide a non-invasive assessment of bone marrow changes in clinical patients undergoing radiotherapy.

© 2014 Published by Elsevier Inc.

1. Introduction

Loss of hematopoietic red marrow is a contributing factor to hematologic toxicity during radiation therapy, and its preservation is one of the goals of intensity-modulated radiation therapy (IMRT) [1,2]. Some of the challenges of IMRT are to identify the areas of bone marrow to be spared and to evaluate the effectiveness of different sparing protocols [3–5].

Magnetic resonance imaging (MRI) is commonly used to assess changes pre- and post-radiation treatment [2,6]. Increased signal intensities on T1-weighted or decreased signal on opposed-phase images has been observed consistently. Such changes are seen in the spine and pelvis following radiation treatment and are consistent with the transformation from hematopoietic red marrow to inactive yellow marrow. While it is plausible that the changes in signal are due entirely to the accumulation of fat, changes in signal on MRI can also be caused by changes in proton density, T1 and T2, as well as scanner calibration and coil positioning. In patients undergoing radiotherapy, the effects of radiation alter the tissue and can change its properties such as T2 [7].

Over the past few years, more sensitive and specific MRI methods have been developed for fat quantification [8]. These do not rely on T1, T2 or T2* but instead use the characteristic proton frequency signature of water and fat molecules (i.e. the chemical shifts). The proton density fat fraction (PDFF) is defined as the fraction of signal from fat protons relative to the signal from all protons and its adoption is encouraged [9]. The converse of PDFF is the proton density water fraction (PDWF = 100% − PDFF), which is the fraction of signal from water protons relative to all protons. While there are other sources of protons in biological tissues, at the time of the MRI measurements (echo time >1 ms) any signal from protons in macromolecues or in rigid arrangements (e.g. connective tissues, minerals) has decayed away. The definition of the PDWF has similarities with the definition of cellularity from histology, which is the fraction of hematopoietic tissue relative to total of hematopoietic and adipose tissues [10].

The medical and scientific community has guidelines for assessing the validity of biological markers (biomarkers) and a stringent process of qualification before accepting a biomarker into clinical practice. Biomarker qualification is the process of establishing the "fitness for purpose" by consensus among groups of scientists and clinicians [11]; the process includes testing robustness, repeatability and reproducibility of the measurement process in clinically relevant situations, and also validation with reference to currently accepted standards (e.g. histology, biochemical assay).

* Corresponding author. Tel.: +1 619 471 0520; fax: +1 619 471 0503.
E-mail address: mbydder@ucsd.edu (M. Bydder).

http://dx.doi.org/10.1016/j.mri.2014.03.005
0730-725X/© 2014 Published by Elsevier Inc.

The objective of this study is to contribute toward the process of qualification of PDWF as a measure of bone marrow cellularity. Whereas cellularity measurements require extraction of bone marrow tissue and cannot generally be justified in patients, the PDWF is a relatively safe, non-invasive measurement. The potential for assessing cellularity by MRI has important clinical applications, including radiation therapy planning to spare areas of high cellularity red marrow and to monitor changes in the bone marrow [4].

2. Methods

2.1. Samples

Fresh, excised spine samples comprising four to eight intact lumbar and thoracic vertebrae were obtained within 72 hours of death of the donor. Donors represent a cross-section from 15 males and 3 females ($n = 18$ total) and were obtained consecutively; mean age 56.3 years (standard deviation 10.1, range 37–75). The causes of death were cardiac-related ($n = 11$), respiratory ($n = 3$), traumatic brain injury ($n = 3$) and renal failure ($n = 1$).

Specimens were either scanned immediately ($n = 8$) or frozen ($n = 10$) and imaged at room temperature up to 6 months later. Frozen specimens were kept in a biohazard bag at −70 °C in an ultralow freezer (Bio-Freezer; Forma Scientific, Marietta, OH, USA).

2.2. MRI technique

Imaging was performed on an MRI 3.0 T HDx scanner (GE Healthcare, WI) using an ankle coil. Specimens were at room temperature. The imaging sequence was an investigational prototype from the manufacturer called IDEAL IQ, which was based on previous methods [12,13]. The acquisition was a sagittal 3D volume, spoiled gradient echo with “Minimum” repetition time (TR) and “Minimum Full” echo time (TE). The approximate values were TR 10 ms and TEs 1.2, 2.2, 3.3 ms etc. acquired in three interleaves with an echo train length of 2 (total of 6 echos). Other settings were: flip angle 2°, bandwidth ±100 kHz, matrix 192 × 192, slice thickness 3 mm, field of view 18–22 cm and 2 averages. Scan times were 3–4 minutes.

2.3. Histological analysis

Imaging results were used to identify two vertebral bodies from each donor, subject to the following exclusion criteria: avoid obvious disk disease, disk compression, hemangioma, and Schmorl's deformity. The selected vertebral bodies were cut axially to obtain a 1-cm section of the center of the marrow. Fatty corners and basilar veins in the vertebral bodies were avoided. The 1-cm sections were then frozen, as described above.

Samples underwent histological slide preparation using a tissue processor (Thermo Scientific Shandon Excelsior). Fixation: core biopsies were placed in 10 to 20 mL of fixative (neutral-buffered formalin) for 18–24 hours. Decalcification: cores were removed from fixative and rinsed with several changes of water for 3 minutes, placed in Decal Stat (Decal Chemical Corp., Tallman, NY) for 1 hour, washed in several changes of water for 5 minutes, placed in 10% neutral-buffered formalin and processed in an automatic tissue processor. Sectioning: paraffin-embedded core biopsies were sectioned in thicknesses of 3–4 μm with coverage of the diameter of the excised vertebral body. Staining: routine hematoxylin–eosin (H&E).

The bone marrow cellularity was determined by a pathologist reading by subtracting the cleared out fatty areas from the total area (the background hematopoietic cells and the background fat cells) and estimated to the nearest 10%.

2.4. Biochemical analysis

A 1- to 2-g sample of the same section was powdered under liquid nitrogen and submitted to AniLytics Inc. (Gaithersberg, MD) for the following tests: water content (given as a percentage of the total mass), triglyceride and total lipid (in units of milligrams per gram of tissue). Further details on the tests may be requested from the company (http://www.anilyticsinc.com/).

An average fat content (of the triglyceride and total lipid assays) was calculated as follows: Fat (%) = 0.1 × (Total Lipid + Triglyceride)/2. This is just the average of the two measurements, expressed as a percentage rather than in units of mg/g.

2.5. MRI analysis

Computation of the PDFF was performed on the scanner using manufacturer-supplied software. Briefly, the IDEAL IQ technique corrects for confounding effects such as $T2^*$ decay, multiple fat peaks, eddy currents and noise bias. The PDFF maps were exported to an Osirix DICOM viewer [14] to manually draw regions of interest (ROIs). The plane was reformatted to axial to match the orientation and thickness of the excised portion of marrow. Avoidance structures for drawing ROIs were fatty corners. The water fraction was calculated using the formula PDWF = 100% − PDFF (in units of %).

2.6. Statistical analysis

Regression analysis was performed in MATLAB version 2011b (The Mathworks, Natick, MA) using the *regress* command. When present, uncertainty ranges represent the 95% confidence interval. Of a total of 180 independent data points, 3 were considered outliers and were excluded from the analysis: (1) the highest total lipid value (531 mg/g) was substantially higher than any other total lipid value and differed from the triglyceride regression line by more than six standard deviations; (2 + 3) two cellularity readings of 30% were noted by the pathologist as having “increased erythroids, serous-like changes” and exhibited the highest water content values (63.4% and 60.9%).

3. Results

Fig. 1 shows an example of the MRI-acquired sagittal PDFF maps and a reformatted axial slice. Indicated on the axial slice is the region of interest from which the mean PDFF was obtained. These can be visualized on the PDFF maps as being 56.9%, resulting in a PDWF of 43.1%. Fig. 2 shows the histological slide matching the images from Fig. 1. The cellularity assessed on this H&E histology slide is 30%.

Fig. 3 contains the quantitative results from biochemical assay and MRI. Panel A shows a Bland–Altman plot for the biochemical assays for triglyceride and total lipid; the very small difference between the two quantities indicates that, within error, all lipids in the samples are present as triglyceride. This finding is consistent with a previous study that reported that adipose tissue is predominantly triglyceride [15]. For the remainder of the study, the lipid and triglyceride are combined into an average Fat (%) content, defined in Methods.

Panel B shows the relation between the biochemical water and fat assays. If the samples were composed entirely of water and fat then they should sum to 100%, however this is not observed. The plot shows that water represents only 55.0% of the mass as the fat content approaches zero. The remaining 45.0% of the mass is presumably mineral and protein associated with trabecular structure. Using the linear regression from the plot, Water = 55.0 − 0.544 × Fat, it can be calculated that when the water content approaches zero the fat content approaches 55.0/0.544 ≈ 101.1% (i.e. all of the mass).

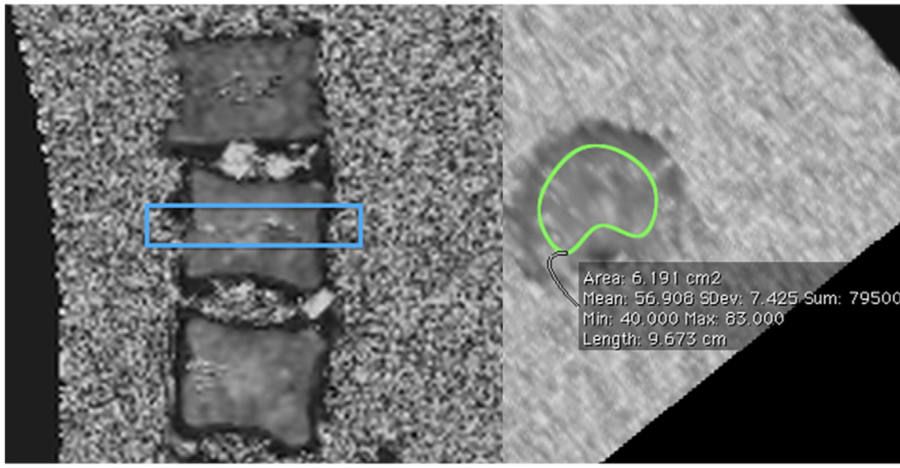

Fig. 1. Examples of PDFF maps of an intact spine specimen produced by IDEAL IQ. The sagittal volume was reformatted to axial plane and regions of interests were drawn inside the vertebral bodies, as indicated, avoiding fatty corners. The mean PDFF was recorded (in this case 56.9%) and the PDWF calculated from 100 − PDFF (in this case 43.1%).

This implies that the mineral and protein content must approach zero.

Panel C shows a strong positive correlation between PDFF and fat content from biochemical assay ($r = 0.77$). The PDFF is a measure of the MRI-visible fat protons relative to the total number of MRI-visible protons and the biochemical assay detects all mass present in the form of fat. A positive intercept indicates that a quantity of fat protons is MRI invisible, however this could be considered negligible since it is zero within the 95% confidence interval (2.99 ± 5.21). The slope is significantly different from unity (0.406 ± 0.115).

Consider that the sample is made up of four compartments: water (W), fat (F), minerals and proteins (MP). The latter are invisible on MRI so the fat content by MRI (assuming all other sources of error have been removed) is $F/(F + W)$ whereas the fat content by mass is $F/(F + W + \mathrm{MP})$. The non-unity slope in panel C indicates that the mass of MP is a significant fraction of the denominator; however this is complicated by the possibility that MP may vary with fat content (panel B). A second issue of relevance to the non-unity slope is that the number of protons in a sample does not in general have a simple relationship to the mass; for water and triglyceride the conversion factor is close to unity [9].

Panel D shows a strong positive correlation between PDWF and water content from biochemical assay ($r = 0.76$). As with panel D, a positive intercept indicates the presence of MRI-invisible water protons and in this case it is significantly different from zero (20.3 ± 7.1). It is reasonable to expect a proportion of the water to be bound to proteins in the sample and therefore be undetectable by standard MRI techniques.

Fig. 4 shows the quantitative results involving cellularity. Panel A reveals a strong correlation between PDWF and cellularity ($r = 0.72$). Panel B finds a correlation between water content and cellularity ($r = 0.56$). The positive intercepts on both plots clearly indicate that a percentage of the water content is not cellular (approximately 32.0%).

4. Discussion

The present study has found correlations between biochemical, histological and MRI-derived measures of water and fat content in ex vivo spine bone marrow (Table 1). The principal finding, shown in Fig. 4A, is that the cellularity is strongly correlated with the proton density water fraction (PDWF) as measured by MRI. The clinical value of this result is that the cellularity can be estimated from non-invasive

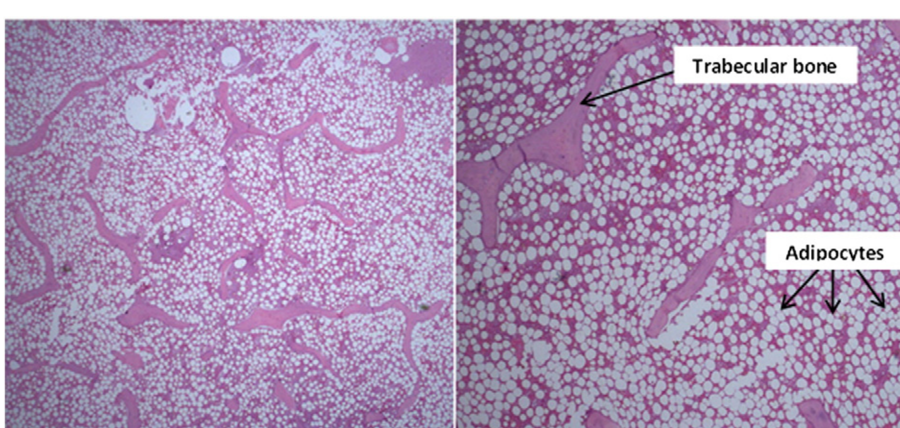

Fig. 2. Example of histological slides using the same sample as Fig. 1, shown at low and high magnifications. In this sample the cellularity was 30%, the PDWF was 43.1% and the biochemical water assay was 39%.

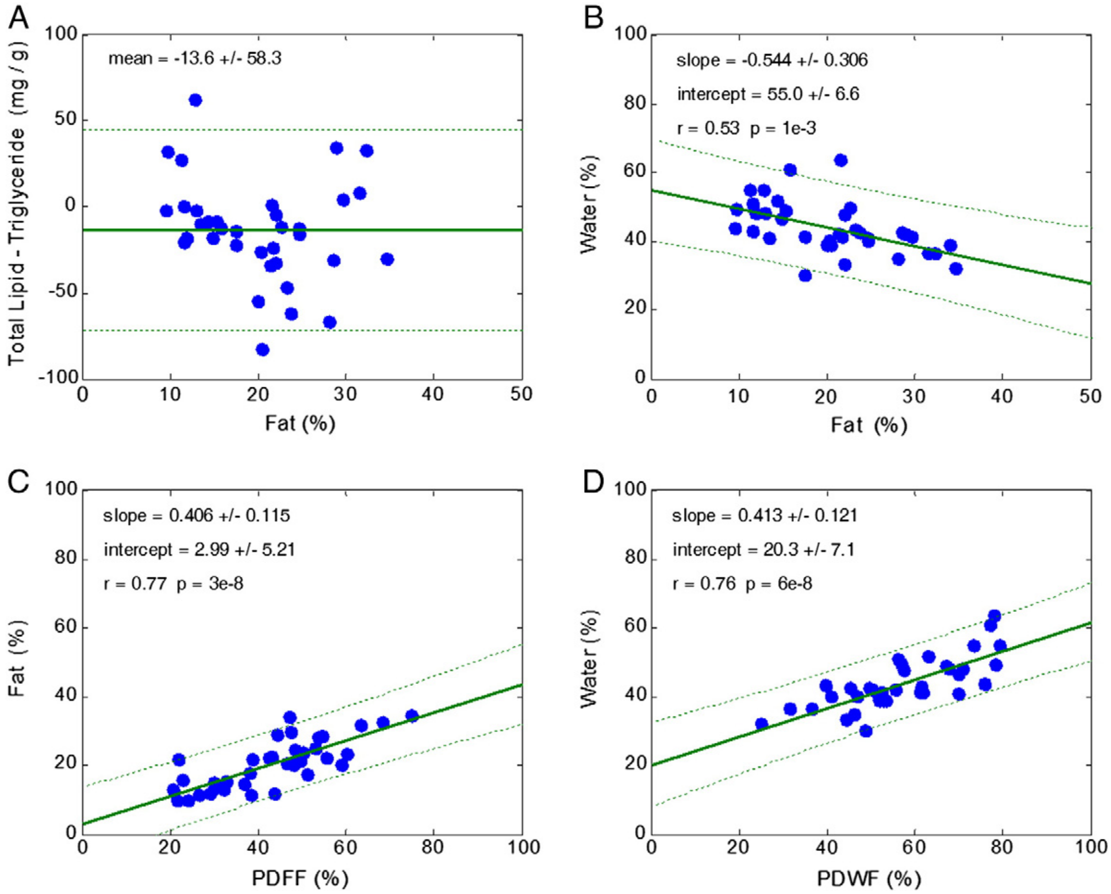

Fig. 3. Bland–Altman and correlation plots for total lipid, triglyceride, proton density water fraction (PDFF), proton density fat fraction (PDFF) and water content. Regression lines and coefficients are shown with the 95% prediction intervals and 95% confidence intervals.

MRI, which facilitates longitudinal monitoring of disease progression and/or response to radiotherapy. Quantitation provides objective information upon which clinical decisions can be made.

The findings suggest that cellularity can be predicted from the PDWF by the following relation: Cellularity $= 25.5 + 0.633 \times$ PDWF (%). The non-zero intercept (25.5%) indicates that a percentage of the water in the sample is non-cellular. Comparison of cellularity with water content measured by biochemical assay (Fig. 4B) also indicates the presence of non-cellular water (intercept 32.0%); the slightly higher value from biochemical assay may indicate the presence of so-called MRI-invisible water protons, such as those bound to protein [16]. Non-cellular water in the bone marrow may be due to serous changes or edema.

Another finding from biochemical assay is that the lipid in bone marrow is essentially all in the form of triglyceride, in agreement with a previous study [15]. The Bland–Altman plot in Fig. 3A shows that the difference between the mass of all lipids and the mass of triglycerides is zero within error. This is useful for modeling the

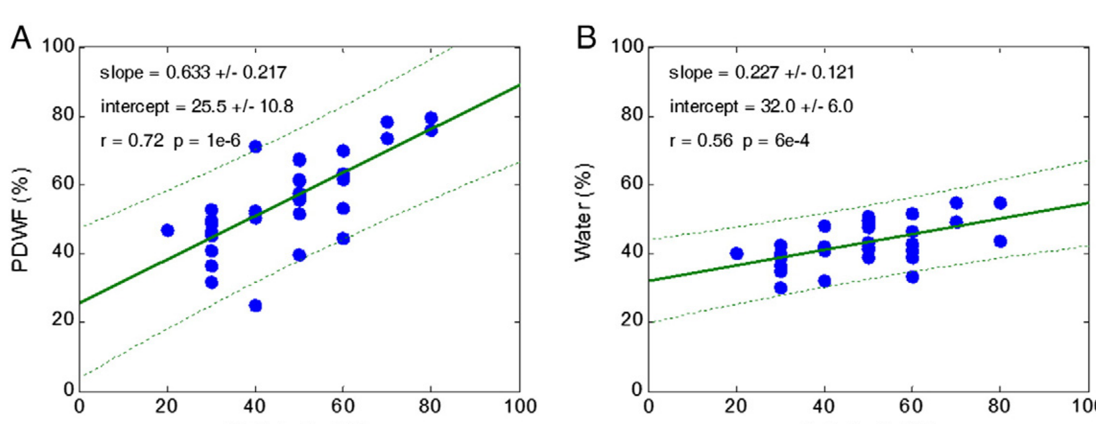

Fig. 4. Correlation plots of the cellularity versus proton density water fraction (PDFF) and water content from biochemical assay. Regression lines and coefficients are shown with the 95% prediction intervals and 95% confidence intervals.

Table 1
Summary of the correlations measured in the present study.

Test	Correlation coefficient
Total lipid vs triglyceride	0.96
Fat vs PDFF	0.77
Water vs PDWF	0.76
PDWF vs cellularity	0.72
Water vs cellularity	0.56

signal in MRI fat quantification techniques [17], since any signal from non-triglyceride lipids (e.g. free fatty acids, phospholipids, cholesterol) can be considered negligible.

Evidence from the present study suggests that up to 45.0% of the mass in bone marrow is non-water and non-fat (Fig. 3B), most likely from trabecular minerals and proteins. It is interesting that this percentage decreases with increasing fat content, implying that fatty marrow is associated with reduced trabecular bone mass. A similar relation between bone density and fat content has been reported previously using different methodology [18].

Measuring correlation between modalities is key step in the qualification of biomarkers [11]. Finding a strong correlation gives confidence that different techniques are measuring the same physical quantity (i.e. the fat or water content in the tissue). However, the units of these measures are fundamentally different; PDFF measures the proton abundance, biochemical assay measures the mass and histology measures the cell area on a slide. The PDFF can be converted to the fraction by mass or by volume of tissue [9,19] although MRI-invisible mass is neglected in this conversion. Non-zero intercepts and non-unit slopes in several of the correlation plots are indicative of the differences in physical units. Also, the relation between water content and cellularity may break down with certain pathologies. Such effects were apparent in samples with serous changes (rejected as outliers), where the cellularity was at the lowest end of the range but the water content was at the highest.

The present study has several limitations. The sample size of 36 vertebral bodies from 18 donors was small, although sufficient to detect significant correlations between the different fat and water measurements. The range of fat content was determined by the population sample and matched the typical range in of cellularity in bone marrow of 30%–70%. Obtaining samples outside this range may strengthen the correlation, or possibly may introduce non-cellular water content that would weaken the correlation.

Acknowledgments

Support for this project was provided by GE Healthcare and NIH grant R21 (No. CA162718).

References

[1] Kirwan JM, Symonds P, Green JA, Tierney J, Collingwood M, Williams CJ. A systematic review of acute and late toxicity of concomitant checbemoradiation for cervical cancer. Radiother Oncol 2003;68:217–26.
[2] Addley HC, Vargas HA, Moyle PL, Crawford R, Sala E. Pelvic imaging following chemotherapy and radiation therapy for gynecologic malignancies. RadioGraphics 2010;30:1843–56.
[3] Mell LK, Kochanski JD, Roeske JC, Haslam JJ, Mehta N, Yamada SD, et al. Dosimetric predictors of acute hematologic toxicity in cervical cancer patients treated with concurrent cisplatin and intensity-modulated pelvic radiotherapy. Int J Radiat Oncol Biol Phys 2006;66(5):1356–65.
[4] Liang Yun, Bydder Mark, Yashar Catheryn M, Rose Brent S, Cornell Mariel, Hoh Carl K, et al. Prospective study of functional bone marrow-sparing intensity modulated radiation therapy with concurrent chemotherapy for pelvic malignancies. Int J Radiat Oncol Biol Phys 2013;85(2):406–14.
[5] Rose BS, Liang Y, Lau SK, Jensen JG, Yashar CM, Hoh CK, et al. Correlation between radiation dose to 18F-FDG-PET defined active bone marrow subregions and acute hematologic toxicity in cervical cancer patients treated with chemoradiotherapy. Int J Radiat Oncol Biol Phys 2012;15(83):1185–91.
[6] Casamassima F, Ruggiero C, Caramella D, Tinacci E, Villari N, Ruggiero M. Hematopoietic bone marrow recovery after radiation therapy: MRI evaluation. Blood 1989;73(6):1677–81.
[7] Argiris A, Maris T, Papavasiliou G, Gouliamos A, Papavasiliou C. Radiotherapy effects on vertebral bone marrow: easily recognizable changes in T2 relaxation times. Magn Reson Imaging 1996;14(6):633–8.
[8] Hu HH, Börnert P, Hernando D, Kellman P, Ma J, Reeder S, et al. ISMRM workshop on fat-water separation: insights, applications and progress in MRI. Magn Reson Med 2012;68(2):378–88.
[9] Reeder Scott B, Hu Houchun H, Sirlin Claude B. Proton density fat-fraction: a standardized MR-based biomarker of tissue fat concentration. J Magn Reson Imaging 2012;36(5):1011–4.
[10] Bain BJ, Clark DM, Lampert IA. Bone marrow pathology. 3rd ed. Blackwell Science; 2001. p. 8.
[11] Waterton JC. What imaging biomarkers are and how they are used. Proceedings of the International Society of Magnetic Resonance in Medicine, Educational Lectures; 2009.
[12] Yu H, Shimakawa A, McKenzie CA, Brodsky E, Brittain JH, Reeder SB. Multiecho water-fat separation and simultaneous R2* estimation with multifrequency fat spectrum modeling. Magn Reson Med 2008;60:1122–34.
[13] Yu H, Shimakawa A, Hines CDG, McKenzie CA, Hamilton G, Sirlin CB, et al. Combination of complex-based and magnitude-based multiecho water-fat separation for accurate quantification of fat-fraction. Magn Reson Med 2011;66:199–206.
[14] Rosset Antoine, Spadola Luca, Ratib Osman. OsiriX: an open-source software for navigating in multidimensional DICOM images. J Digit Imaging 2004;17(3):205–16.
[15] Ren J, Dimitrov I, Sherry AD, Malloy CR. Composition of adipose tissue and marrow fat in humans by 1H NMR at 7 Tesla. J Lipid Res 2008;49(9):2055–62.
[16] Krasnosselskaia LV. Mechanisms for Short T2 and T2* in collagen-containing tissue. In: Bydder GM, Fullerton GD, Young IR, editors. MRI of Tissues with Short T2s or T2*s. 1st ed. United Kingdom: John Wiley & Sons; 2012. p. 31–41.
[17] Hamilton G, Yokoo T, Bydder M, Cruite I, Schroeder ME, Sirlin CB, et al. In vivo characterization of the liver fat ^{1}H MR spectrum. NMR Biomed 2011;24(7):784–90.
[18] Griffith JF, Yeung DK, Antonio GE, Lee FK, Hong AW, Wong SY, et al. Vertebral bone mineral density, marrow perfusion, and fat content in healthy men and men with osteoporosis: dynamic contrast-enhanced MR imaging and MR spectroscopy. Radiology 2005;236(3):945–51.
[19] Bydder M, Girard O, Hamilton G. Mapping the double bonds in triglycerides. Magn Reson Imaging 2011;29(8):1041–6.